SLAC-PUB-952
(TH) and (EXP)
August 1971

PROPERTIES OF HADRONIC AMPLITUDES IN AN ABSORPTIVE MODEL†

Haim Harari* and Adam Schwimmer*
Stanford Linear Accelerator Center, Stanford University, Stanford, California 94305

ABSTRACT

Hadronic two-body amplitudes involve two components. The imaginary part of the nondiffractive component R is dominated by the most peripheral impact parameters ($b \sim r$). The imaginary part of the diffractive component P has substantial contributions from all impact parameters $b \lesssim r$. We study the energy dependence of the b-representations of both components as well as various possible forms for the corresponding real parts. We show that the following three assumptions are mutually inconsistent: (i) Im R(s, t) is always dominated by $b \sim r$ terms; (ii) Im R(s, t) shrinks indefinitely as $s \to \infty$, (iii) r approaches a constant as $s \to \infty$. We define three classes of models obtained by abandoning, one at a time, these three assumptions. We discuss the complex J-plane structure as well as the asymptotic phase of the R-amplitude for each of these classes and propose various experimental ways of distinguishing between the models. A detailed analysis of Re R indicates that, while in certain cases it reaches its asymptotic phase at relatively low energies, in other cases the asymptotic phase is approached very slowly and it has no resemblance to the observed phase at present energies.

---

† Supported by the U. S. Atomic Energy Commission.

* On leave of absence from the Weizmann Institute of Science, Rehovot, ISRAEL.

(Submitted to Phys. Rev.)

I. Introduction

The phenomenological description of hadronic scattering amplitudes for two-particle final states involves two components.[1] The first component, R(s, t), contributes to both elastic and inelastic processes. According to the usual duality ideas[2] it can be viewed either as a sum of s-channel resonances or as a combination of "ordinary" t-channel exchanges (poles and cuts). The second component, P(s, t), is the diffractive "Pomeron-exchange" part and it contributes only to elastic (or quasielastic) processes.

Both the t-channel and the s-channel points of view seem to be crucial for the description of various systematic features of elastic and inelastic amplitudes. In general, the t-channel picture has been more successful in explaining the s-dependence of hadronic amplitudes while the s-channel picture has been very useful in understanding the structure of amplitudes as a function of t.

Many systematic features of the t-dependence of differential cross-sections can be successfully explained in terms of a simple dual absorptive picture which relies heavily on an s-channel impact parameter description of the amplitude. According to this picture[3], the impact parameter representation of Im R(s, t) is dominated, at energies of several BeV's, by the most peripheral impact parameters within the interaction radius[4-8] (figure 1a). The analogous representation of Im P(s, t) includes substantial contributions for all impact parameters within a certain radius (figure 1b). We believe that this qualitative description is correct at energies between, say, 2 and 20 BeV. Whether it continues to hold at higher energies, we do not know. The development with energy of the two functions of figure 1 is obviously a crucial question which has to be tackled before we can make any progress in understanding the features of hadronic two body reactions at higher

energies. In fact, once we accept the general features of figure 1, the following set of problems becomes relevant:

(i) The functions of figure 1 can be presumably characterized by a few parameters such as the effective interaction radius (which may be different for the R and P amplitudes), the value of the amplitude at the peak and the width of the peripheral R-amplitude. How do these parameters vary with energy? Do we have a fixed width? fixed radii?

(ii) Given an answer to the previous question, how do we translate the resulting amplitude into the language of t-channel exchanges and singularities in the complex angular momentum plane?

(iii) Given the impact parameter representation of Im R and Im P at all energies, what can we say about the real parts of these amplitudes?

(iv) What is the physical interpretation of the various possible answers to the previous questions? What (if any) is the relation between these possibilities and the existing models for hadronic reactions?

(v) Which future experiments can distinguish between the different possibilities?

In the present paper we address ourselves to all of these questions. In Section II we discuss several possible schemes for the energy dependence of Im R. We discuss three classes of models —

(I) Models in which peripheral dominance is abandoned at high energies.

(II) Models in which shrinking stops at high energies.

(III) Models in which the radius increases with energy.

The first two classes correspond to certain moving pole schemes and fixed singularity schemes, respectively. The third class of models corresponds to a more complicated J-plane structure involving complex singularities.

Section III is devoted to a brief discussion of experimental ways of distinguishing between the three classes of models.

In Section IV we investigate the real part of the R-amplitude within the framework of our models.

A few applications and tests of these real parts are presented in Section V.

In Section VI we compare our ideas with previous models and briefly discuss the classification of these models into our three classes.

Section VII is devoted to an analysis of the P-component, its energy dependence and its real part.

Our main conclusions are summarized in Section VIII.

II. Energy Dependence of the Impact Parameter Description of Im R(s, t)

Our basic assumption is that, at energies of several BeV's, Im R(s, t) is dominated by the peripheral impact parameters. The impact parameter representation $\mathscr{R}(s, b)$ of an s-channel helicity amplitude R(s, t) is given by the usual Bessel transform:

$$\mathscr{R}(s, b) = \int_0^\infty R(s, t) J_{\Delta\lambda}(b\sqrt{-t})\sqrt{-t}\, d\sqrt{-t} \qquad (1)$$

where $\Delta\lambda$ is the total s-channel helicity change.

If the strength of $\mathrm{Im}\,\mathscr{R}(s, b)$ is entirely concentrated at a point b = r, namely —

$$\mathrm{Im}\,\mathscr{R}(s, b) \propto \delta(b-r) \qquad (2)$$

we obviously have:

$$\mathrm{Im}\,R(s, t) \propto J_{\Delta\lambda}(r\sqrt{-t}) \qquad (3)$$

A more realistic case would be to consider an impact parameter representation which is peaked at $b \sim r$ but has a finite width around this point. In such a case the $J_{\Delta\lambda}(r\sqrt{-t})$-factor in the t-representation will be multiplied by a smooth function such as e^{At}. In order to simplify our analysis, we shall therefore explicitly discuss amplitudes whose t-dependence is given by —

$$\text{Im}\, R(t) = C\, e^{At} J_{\Delta\lambda}(r\sqrt{-t}) \tag{4}$$

All of our results, however, apply to a much wider class of amplitudes, namely — to all amplitudes whose b-representation is clearly dominated by the region $b \sim r$. The particular amplitude of Eq. (4) corresponds to[9]:

$$\text{Im}\, \mathscr{R}(b) = \frac{C}{2A}\, e^{-\frac{r^2+b^2}{4A}}\, I_{\Delta\lambda}\left(\frac{rb}{2A}\right) \tag{5}$$

where $I_{\Delta\lambda}$ is the hyperbolic Bessel function $\left[I_{\Delta\lambda}(x) = J_{\Delta\lambda}(ix)\right]$. Using the asymptotic expansion[9] of $I_{\Delta\lambda}(x)$ —

$$I_{\Delta\lambda}(x) = \frac{e^x}{\sqrt{2\pi x}}\left[1 + O\left(\frac{1}{x}\right)\right] \tag{6}$$

we can approximate $\mathscr{R}(b)$, for $b > \frac{2A}{r}$, by:

$$\text{Im}\, \mathscr{R}(b) = \frac{C}{2\sqrt{\pi A r b}}\, e^{-\frac{(r-b)^2}{4A}}\left[1 + O\left(\frac{2A}{rb}\right)\right] . \tag{7}$$

The expression (7) exhibits a peak for:

$$b_{max} = r\left[1 + O\left(\frac{A}{r^2}\right)\right] \tag{8}$$

and the "width" Δ of the peak may be characterized by —

$$\Delta \sim 2\sqrt{A} \tag{9}$$

The value of $\mathscr{R}(b)$ at the peak is:

$$\text{Im}\,\mathscr{R}(b_{max}) = \frac{C}{2r\sqrt{\pi A}}\left[1+O(\frac{A}{r^2})\right] \tag{10}$$

Figure 2 shows the general behavior of such a function. In the t-representation, C determines the overall normalization, r determines the positions of zeroes (and consequently, the positions of dips and crossover effects in angular distributions) and A measures the deviation of the amplitude from a pure Bessel function $J_{\Delta\lambda}(r\sqrt{-t})$. For helicity nonflip ($\Delta\lambda = 0$) the slope of the amplitude at $t = 0$ is determined by r and A:

$$\frac{d}{dt}\left[C\, e^{At} J_0(r\sqrt{-t})\right]_{t=0} = A + \frac{r^2}{4} \tag{11}$$

In the b-representation (to lowest order in A/r^2), r determines the position of the maximum, A reflects the "width", i. e. the degree of localization of the dominant contribution around $b \sim r$ and C fixes the overall magnitude.

The three parameters C, A and r are presumably sufficient for a semi-qualitative description of Im R(s, t) at energies of a few BeV. However, every one of these parameters is, apriori, a function of energy. The energy dependence of C, A and r determines which features of our qualitative picture remain true as the energy increases. Only a study of the functions C(s), A(s) and r(s) may enable us to analyse the features of the non-Pomeron parts of hadronic two-body amplitudes at energies of several hundred BeV.

In the most naive geometrical picture one would tend to assume that the radius r approaches a constant value at high energy:

$$r(s) \xrightarrow[s \to \infty]{} r_\infty \tag{12}$$

In this case a shrinkage of R(s, t) (as observed, for instance, in $\frac{d\sigma}{dt}(\pi^- p \to \pi^o n)$) can come only from an increasing A(s). In particular, the usual logarithmic shrinkage implies[10]:

$$A(s) \xrightarrow[s \to \infty]{} A_0 \log s \tag{13}$$

However, the condition for a dominant peripheral contribution is:

$$\sqrt{A(s)} < r(s) \tag{14}$$

(i. e. the width of the peak in figure 1a should be sufficiently small compared with the radius). The three relations (12), (13) and (14) are, of course, incompatible. We therefore conclude that the following set of assumptions is internally inconsistent:

(i) Dominance of the peripheral partial waves at all energies.

(ii) Indefinite shrinking of non-Pomeron amplitudes at high energies.

(iii) A radius which approaches a constant at high energies.

Facing such an inconsistency, we have to abandon at least one of these three assumptions. We are led to three alternative classes of models for the behavior of non-Pomeron amplitudes at high energies.

Class I models: We first consider models in which we abandon assumption (i), namely — we do not insist that the peripheral partial waves always dominate. We have[10]:

$$r(s) \xrightarrow[s \to \infty]{} r_\infty; \quad A(s) \xrightarrow[s \to \infty]{} A_0 \log s \tag{15}$$

$$\text{Im } R(s,t) \xrightarrow[s \to \infty]{} C(s)\, s^{A_0 t}\, J_{\Delta\lambda}(r_\infty \sqrt{-t}) \tag{16}$$

In this case, when the energy increases, the amplitude "will lose its peripherality" and the significant $b \sim r$ peak of $\text{Im } \mathcal{R}(s,b)$ will disappear at high energies. Figure 3 shows typical b-representations for relatively large values of A. The characteristic properties of such a model include:

(i) Dips and crossover effects which are fixed in t.

(ii) Indefinite shrinkage of differential cross sections.

(iii) At sufficiently large energy the dips will become less and less significant as a result of the increased slope (in other words — the relative strength of the secondary peak and the first peak in the angular distribution becomes smaller).

An example of such a model is an ordinary Regge pole model with a residue function of the form $J_{\Delta\lambda}(r_\infty \sqrt{-t})$. In such a model[10,11]:

$$C(s) \xrightarrow[s \to \infty]{} C_0 s^{\alpha_0} \tag{17}$$

and

$$\text{Im } R(s,t) \xrightarrow[s \to \infty]{} C_0 s^{\alpha_0 + A_0 t} J_{\Delta\lambda}(r_\infty \sqrt{-t}) \tag{18}$$

A typical Regge model will, however, require ghost killing factors which are (in general, but not always) inconsistent with our $J_{\Delta\lambda}(r_\infty \sqrt{-t})$ residue function. We shall return to this point in Section IV, in our discussion of the real part.

Class II models: In the second class of models we abandon the assumption of indefinite shrinkage. We then have —

$$r(s) \xrightarrow[s\to\infty]{} r_\infty ; \quad A(s) \xrightarrow[s\to\infty]{} A_\infty \tag{19}$$

$$\text{Im } R(s,t) \xrightarrow[s\to\infty]{} C(s)\, e^{A_\infty t} J_{\Delta\lambda}(r_\infty \sqrt{-t}) \tag{20}$$

In this case the dominance of the peripheral partial waves can be maintained at all energies (provided that $\sqrt{A_\infty} < r_\infty$). The entire energy dependence is given by C(s) and the shape of the angular distribution "freezes" at high energies. The characteristic experimental consequences of such a model involve:

(i) Dips and crossover effects at fixed t-values.

(ii) No shrinking at high energies.

(iii) An identical energy dependence for any fixed t.

Models of this category correspond to fixed t-channel singularities (poles or cuts) in complex angular momentum plane.

Class III models: Finally we consider the possibility that the radius r(s) is not constant at high energies. In this case, if r(s) increases at least as fast as $[A(s)]^{\frac{1}{2}}$, we may have indefinite shrinking and maintain the dominance of the peripheral impact parameters as $s \to \infty$. A typical example of such a model would be

$$r(s) \xrightarrow[s\to\infty]{} r_0 \log s ; \quad A(s) \xrightarrow[s\to\infty]{} A_0 \log s \tag{21}$$

$$\text{Im } R(s,t) \xrightarrow[s\to\infty]{} C(s)\, e^{A_0 t \log s} J_{\Delta\lambda}(r_0 \log s \sqrt{-t}) \tag{22}$$

If we further assume that C(s) follows a power behavior we have:

$$C(s) \xrightarrow[s\to\infty]{} C_0 s^{\alpha_0} \tag{23}$$

$$\text{Im } R(s,t) \xrightarrow[s\to\infty]{} C_0 s^{\alpha_0 + A_0 t} J_{\Delta\lambda}(r_0 \log s \sqrt{-t}) \tag{24}$$

A slight variation of this model would replace r(s) in Eq. (21) by:

$$[r(s)]^2 \xrightarrow[s\to\infty]{} r_0^2 \log s \tag{25}$$

This is the usual energy dependence of the effective radius in most Reggeistic models. In that case the arguments of the Bessel functions in Eqs. (22) and (24) will be modified. Equation (24) would then read:

$$\text{Im } R(s,t) \xrightarrow[s\to\infty]{} C_0 s^{\alpha_0 + A_0 t} J_{\Delta\lambda}(r_0 \sqrt{-t \log s}) \tag{26}$$

The most obvious experimental characteristics of this class of models are:

(i) As the energy increases, the positions of dips and crossover effects in angular distributions should generally shift towards smaller t-values.

(ii) Inelastic differential cross sections should shrink indefinitely.

(iii) The energy dependence of any given amplitude at fixed t (but not at t = 0) will show oscillations as a result of the moving zeroes.

In order to analyze this type of model in terms of its singularities in the complex J-plane we may use the integral representation[9] for $J_{\Delta\lambda}$.

$$J_{\Delta\lambda}(x) = \frac{1}{2\pi} \int_{-\pi}^{+\pi} e^{ix \sin\phi - i\phi\cdot\Delta\lambda} \, d\phi \ . \tag{27}$$

Equation (24) will then take the form:

$$\text{Im } R(s,t) \xrightarrow[s\to\infty]{} \frac{C_0}{2\pi} s^{\alpha_0 + A_0 t} \int_{-\pi}^{+\pi} s^{i \sin\phi \, r_0 \sqrt{-t}} e^{-i\phi\Delta\lambda} d\phi \ . \tag{28}$$

We obtain a superposition of complex poles at

$$J = \alpha_0 + A_0 t + i \sin\phi \, r_0 \sqrt{-t} \tag{29}$$

For all $-1 \leq \sin\phi \leq +1$. Our class III model is therefore reflected in the complex J-plane by the unpleasant structure of a complex conjugate pair of moving branch points[12] (see figure 4) at:

$$\alpha_{\pm}(t) = \alpha_0 + A_0 t \pm i r_0 \sqrt{-t} \tag{30}$$

The actual J-plane structure may be even more complicated if we admit log s terms into the expression (23) for C(s).

The characteristic properties of the three classes of models are summarized in table I. It is clear that other possibilities exist, in which two (or all three) of our basic properties (peripheral dominance, indefinite shrinking, constant radius) are abandoned. Since we are reluctant to give up even one of them, we believe that such "exotic" models are not very realistic.

III. The Imaginary Part of R(s, t): Proposed Experimental Tests

In order to find which one of our three classes of models actually describes Im R(s, t) we must determine the high energy behavior of r(s) and A(s). We have remarked in the previous section that, at any given energy, r determines the positions of the zeroes of the various imaginary parts while both r and A appear in the expression for the slope of the amplitude. Consequently, it is simpler to isolate the s-dependence of the radius r.

The energy dependence r(s) can best be studied by finding the t-values in which dips and crossover effects occur. The most direct test involves the position of the crossover point between particle and antiparticle elastic differential cross sections on the same target. It is well known that the quantity $\left[\frac{d\sigma}{dt}(\bar{x}p) - \frac{d\sigma}{dt}(xp)\right]$, for $x = \pi^+, K^+, p$, changes sign somewhere around $t \sim -0.2$ BeV^2 at energies of several BeV's. Since the Pomeron contributes equally to xp and $\bar{x}p$ elastic scattering the most important term in the different between the two cross sections is the interference term:

$$\frac{d\sigma}{dt}(\bar{x}p) - \frac{d\sigma}{dt}(xp) \sim 2 \operatorname{Im} P(s,t) \operatorname{Im} R_0(s,t) \quad . \tag{31}$$

The expression (31) vanishes wherever $J_0(r\sqrt{-t})$ does[3] and the t-value of its first zero determines the argument of this Bessel function and hence the value of r. If r(s) is constant, the crossover point should remain at a fixed t-value at all energies. If r increases logarithmically, the crossover point should move slowly towards lower t-values, as the energy increases. Experiments at NAL should be able to settle this point. A rough estimate indicates[13] that if the crossover point moves at all, it should move by about 0.05 - 0.1 BeV^2 in t between, say, 5 BeV and 200 BeV. The present data below 20 BeV are not sufficiently accurate for such a study. An accurate determination of the crossover t-value requires a knowledge of the exact relative normalization of the particle and antiparticle elastic differential cross sections at the same energy. We hope that in future experiments, a special effort will be made to minimize the experimental ambiguities in these relative normalizations.

Another test of the energy dependence of r(s) is offered by the positions of dips in processes such as $\pi^- p \to \pi^0 n$ or $\gamma p \to \pi^0 p$. Here, again, an increasing radius should lead to a moving dip. The position of any of the inelastic dips should then

move to lower t-values as the energy increases. This effect, if it exists, should also be visible at energies of several hundred BeV.

It is more difficult to study A(s), especially if r(s) is not constant. If the radius stays constant (namely — if the dips and crossover points do not move in t), any shrinking effect must come from increasing A(s). However, if r(s) increases, the only way to study A(s) would be to fit specific amplitudes, as a function of t at different values of s by expressions of the form:

$$\text{Im } R(s,t) = C(s)\, e^{A(s)t} J_{\Delta\lambda}\left[r(s)\sqrt{-t}\right] \tag{32}$$

However, this cannot be done in a model independent way. In order to isolate the imaginary part of a specific helicity amplitude we must make certain assumptions concerning the real part of the same amplitude, the relative strength of different helicity amplitudes and, in some cases, the Pomeron exchange amplitude. Here also, we believe that the best chance for studying A(s) is offered by the quantity $\left[\frac{d\sigma}{dt}(\bar{x}p) - \frac{d\sigma}{dt}(xp)\right]$. More explicitly, we should use the relation[3]:

$$\frac{\frac{d\sigma}{dt}(K^- p) - \frac{d\sigma}{dt}(K^+ p)}{2\sqrt{\frac{d\sigma}{dt}(K^+ p)}} = C(s)\, e^{A(s)t}\, J_0\left[r(s)\sqrt{-t}\right] \tag{33}$$

and study A(s) using elastic differential cross sections at different energies. Again — the present data are not sufficiently accurate for a meaningful analysis.

It is somewhat paradoxical that our best hope for understanding the "inelastic" component of hadronic scattering, R(s, t), and its parameters r(s) and A(s) is in performing accurate measurements of elastic differential cross sections. This curious situation is a consequence of our poor knowledge of the real parts of R-amplitudes. In elastic scattering, the predominantly imaginary P-term projects

out the imaginary part of the $\Delta\lambda = 0$ R-amplitude[3] through their interference term, enabling us to study Im R(s, t) in an almost model independent way.

We hope that accurate measurements of elastic differential cross sections in the crossover region as well as studies of the slope and dip-position of inelastic differential cross sections will soon enable us to distinguish between our three classes of models.

IV. The Real Part of R(s, t): Mathematical Analysis

Our discussion, so far, has been centered around the impact parameter representation of the imaginary part of the R-amplitude. We believe that this imaginary part may have relatively simple properties (namely — the dominance of $b \sim r$ impact parameters) as a result of the simple properties of the prominent s-channel resonances. It is much more difficult to make specific statements concerning the real part of the same amplitude. The contributions of s-channel resonances to the real part are not as localized in energy as the contributions to the imaginary part. Consequently, we have no reason to assume that the simple energy-spin relation ($\ell \propto \sqrt{s}$) which applies to the dominant terms in the imaginary part, is also valid for the real part.[3]

The only way of making intelligent guesses on the behavior of the real part is presumably to deduce it from the t and s dependence of the imaginary part of the same amplitude. If we know the asymptotic energy dependence of Im R(s, t), we can compute the high energy form of Re R(s, t). This follows from several theorems relating the asymptotic energy dependence and the asymptotic phase of hadronic amplitudes.[14] In practice, we can easily determine the $s \to \infty$ limit of Re R(s, t) by inserting the corresponding limit of Im R(s, t) into fixed-t dispersion relations. This would give us the real part, subject to two additional assumptions —

(i) In principle, the amplitude may always include a real constant (in s) which cannot be identified by studying the imaginary part. We will tentatively ignore such a possibility, but we must remember that our conclusions regarding the real part are valid only modulu such an additive constant (for any fixed t).

(ii) In order to study the real part, using fixed t dispersion relations, we have to know the high energy behavior of Im R(s, t) for $s \to \infty$ and for $s \to -\infty$. In order to simplify our discussion we shall use amplitudes with definite signature (in other words — with a definite connection between their $s \to \pm \infty$ limits). We realize that, in general, we may have combinations of different signatures, but this should not modify the essential features of our analysis.[15]

Having made these assumptions, we may now proceed to discuss the real part of R(s, t) within the framework of our three classes of models.

Class I models: We assume that as $s \to \infty$, Im R(s, t) is given by[11]:

$$\text{Im } R(s,t) \xrightarrow[s \to \infty]{} C_0 s^{\alpha_0 + A_0 t} J_{\Delta\lambda}(r_\infty \sqrt{-t}) \quad . \tag{34}$$

The high energy limit of the full (real part and imaginary part of the) amplitude can be determined from its discontinuity (34). For an amplitude $R^{\pm}$ with a definite signature, we find:

$$R^{\pm}(s,t) \xrightarrow[s \to \infty]{} - C_0 J_{\Delta\lambda}(r_\infty \sqrt{-t})\, s^{\alpha(t)}\, \frac{e^{-i\pi\alpha(t)} \pm 1}{\sin \pi \alpha(t)} \tag{35}$$

where

$$\alpha(t) = \alpha_0 + A_0 t \quad . \tag{36}$$

The ratio between the real and imaginary parts is given by:

$$\frac{\mathrm{Re}\, R^{+}(s,t)}{\mathrm{Im}\, R^{+}(s,t)} \xrightarrow[s\to\infty]{} -\cot\frac{\pi\alpha(t)}{2} \tag{37}$$

$$\frac{\mathrm{Re}\, R^{-}(s,t)}{\mathrm{Im}\, R^{-}(s,t)} \xrightarrow[s\to\infty]{} \tan\frac{\pi\alpha(t)}{2} \tag{38}$$

The presence of extra log s terms in C(s) in Im R(s, t) would not change the asymptotic ratios (37) and (38) (except for integer values of $\alpha(t)$; see below). However, the rate of approach to these asymptotic ratios may be logarithmically slow. In such a case, the real part at intermediate energies may remain essentially unpredictable.

A delicate problem arises in this class of models at (integer) α-values for which the ratios (37) and (38) develop poles. The real part of the physical amplitude should obviously be finite for $t < 0$, and some mechanism should therefore eliminate these unwanted poles. The only place where this problem is of practical importance is the $\alpha(t) = 0$ point of the even signatured tensor exchange (where $\alpha(t) \sim 0.5 + t$). The $\alpha(t) = -1$ point of the vector trajectory ($t \sim -1.5$ GeV^2?) is probably well outside the domain of validity of our approximate expressions.

There are several ways by which the $\alpha(t) = 0$ pole of Eq. (37) can be avoided. We mention two of them:

(a) It may happen that $J_{\Delta\lambda}(r_\infty \sqrt{-t})$ vanishes at the t-value corresponding to $\alpha(t) = 0$. This seems to be the case[3] for $J_1(r\sqrt{-t})$ for $r \sim 1$ fermi and $\alpha(t) \sim 0.5 + t$. In such a case, the zero of $J_{\Delta\lambda}$ cancels the pole of $\cot\frac{\pi\alpha(t)}{2}$ and a well-behaved real part results. This mechanism may operate in some cases but it cannot be general. If it applies at all, it applies only to a specific helicity amplitude[16] (such as $\Delta\lambda = 1$, but not $\Delta\lambda = 0$, in the above example), and only for a very special correlation between the value of r_∞ and the t-value corresponding to $\alpha(t) = 0$.

(b) A second possible mechanism may result from log s terms in the asymptotic energy dependence of C(s) in Im R(s, t). In the neighborhood of $\alpha(t) = 0$ such logarithmic terms may significantly change the predicted asymptotic ratio (37) between the real and imaginary parts. The resulting real part at $\alpha(t) = 0$ may depend in a very sensitive way on the details of these logarithmic factors. As we remarked above, the actual behavior of the real part at intermediate energies may then be totally unpredictable. An actual case in which this type of situation occurs[3] seems to be the $\Delta\lambda = 0$ amplitude for $\alpha(t) \sim 0.5 + t$ (as in $\mathrm{Re}\, R_{\Delta\lambda=0}$ in $\pi^- p \to \eta n$).

A third possibility is that the poles of the ratios (37) and (38) are removed from the real α-axis by a logarithmic energy dependence of the radius in Eq. (35). Such a possibility corresponds to class III models and we will investigate it below, when we discuss the real parts of class III amplitudes.

It is difficult to determine which one of these possibilities operates in nature. The most likely possibilities in the case of vector and tensor exchanges are[3] the type (a) mechanism for $\Delta\lambda = 1$ amplitudes (where $J_1(r\sqrt{-t})$ happens to vanish at $t \sim -0.5$) and the type (b) mechanism for $\Delta\lambda = 0$ amplitudes where a large cut contribution is known to exist.

Class II models: In these models we assume that, at sufficiently large s, we have:

$$\mathrm{Im}\, R(s,t) \xrightarrow[s\to\infty]{} C(s)\, e^{A_\infty t} J_{\Delta\lambda}(r_\infty \sqrt{-t}) \quad . \tag{39}$$

In this case the dependences on s and on t factorize and the relation between the real part and the imaginary part is entirely determined by the high energy behavior

of C(s). The resulting Re R/Im R ratio is necessarily independent of t. For

$$C(s) \xrightarrow[s\to\infty]{} C_0 s^{\alpha_0} \tag{40}$$

we have:

$$\frac{\mathrm{Re}\, R^{+}(s,t)}{\mathrm{Im}\, R^{+}(s,t)} \xrightarrow[s\to\infty]{} -\cot\frac{\pi\alpha_0}{2} \tag{41}$$

$$\frac{\mathrm{Re}\, R^{-}(s,t)}{\mathrm{Im}\, R^{-}(s,t)} \xrightarrow[s\to\infty]{} \tan\frac{\pi\alpha_0}{2} \tag{42}$$

Class III models: In such models we have assumed that —

$$\mathrm{Im}\, R(s,t) \xrightarrow[s\to\infty]{} C_0 s^{\alpha_0 + A_0 t} J_{\Delta\lambda}(r_0 \log s\sqrt{-t}) \tag{43}$$

or, using the integral representation for $J_{\Delta\lambda}$:

$$\mathrm{Im}\, R(s,t) \xrightarrow[s\to\infty]{} \frac{C_0}{2\pi} s^{\alpha_0 + A_0 t} \int_{-\pi}^{+\pi} s^{i\sin\phi\, r_0\sqrt{-t}} e^{-i\phi\Delta\lambda}\, d\phi \ . \tag{44}$$

Restricting ourselves, for simplicity, to $\Delta\lambda = 0$, we can now perform a Mellin transform and find:

$$\mathrm{Im}\, R_0(J,t) = \frac{C_0}{\pi} \int_{\alpha_-}^{\alpha_+} \frac{1}{\sqrt{(J'-\alpha_+)(J'-\alpha_-)}} \frac{dJ'}{J-J'} \tag{45}$$

where

$$\alpha_{\pm}(t) = \alpha_0 + A_0 t \pm i r_0\sqrt{-t} \ . \tag{46}$$

The corresponding real part can be obtained by constructing the full amplitude whose discontinuity is given by Eq. (45). We find:

$$R_0^{\pm}(j,t) = -\frac{C_0}{\pi}\int_{\alpha_-}^{\alpha_+}\frac{1}{\sqrt{(J'-\alpha_+)(J'-\alpha_-)}}\,\frac{e^{-i\pi J'}\pm 1}{\sin\pi J'}\,\frac{dJ'}{J-J'} \tag{47}$$

Transforming back to the (s, t) variables, we have:

$$\mathrm{Re}\,R_0^{+}(s,t) = -\frac{C_0}{2\pi}\,s^{\alpha_0+A_0t}\int_{-\pi}^{+\pi}\cot\left[\frac{\pi}{2}(\alpha_0+A_0t+ir_0\sqrt{-t}\sin\phi)\right]s^{\,ir_0\sqrt{-t}\sin\phi}\,d\phi \tag{48}$$

$$\mathrm{Re}\,R_0^{-}(s,t) = \frac{C_0}{2\pi}\,s^{\alpha_0+A_0t}\int_{-\pi}^{+\pi}\tan\left[\frac{\pi}{2}(\alpha_0+A_0t+ir_0\sqrt{-t}\sin\phi)\right]s^{\,ir_0\sqrt{-t}\sin\phi}\,d\phi \tag{49}$$

In order to get a qualitative feeling for the behavior of the real part in Eqs. (48), (49) we may use the following approximate expression[17]:

$$\begin{aligned}\mathrm{Re}\,R_0^{-}(s,t) = C_0\,s^{\alpha_0+A_0t}\Big[&\mathrm{Re}\tan\frac{\pi\alpha_+(t)}{2}\,J_0(r_0\log s\sqrt{-t}) - \\ &-\mathrm{Im}\tan\frac{\pi\alpha_+(t)}{2}\,J_1(r_0\log s\sqrt{-t})\Big]\end{aligned} \tag{50}$$

and a similar expression for $\mathrm{Re}R_0^{+}(s,t)$. $\alpha_+(t)$ was defined in Eq. (46). Comparing this expression with the analogous real part for class I models we find that the energy dependence of the radius r leads to two effects:

(i) The first term of Eq. (50) involves $\mathrm{Re}\tan\frac{\pi}{2}\left[\alpha(t)+ir_0\sqrt{-t}\,\right]$ instead of $\tan\frac{\pi\alpha(t)}{2}$. No poles are found at physical values of t and the problem of infinities in Re R(s, t) does not arise. This is the third mechanism for eliminating such infinities that we mentioned in our discussion of class I models earlier in this section.

(ii) The second term in Eq. (50) is usually smaller than the first one (except where the first term vanishes). This term will shift the positions of zeroes of the real part. The shifted zeroes will not coincide with the zeroes of the imaginary part.

The numerical effects of these extra terms are shown in figure 5 where real parts derived from class I and class III models, respectively, are compared.

Another interesting question concerning the real part of the R-ampltiude is whether or not it is dominated by the peripheral impact parameters $b \sim r$. We have started this section by remarking that Re R(s, t) has no <u>apriori</u> reason to obey the $\ell \propto \sqrt{s}$ relation which, for the imaginary part, yields the dominance of the $b \sim r$ impact parameters. Now that we have presented the explicit expressions for the real part within the framework of the three classes of models (and assuming tentatively that the asymptotic phases are reached at an early stage) we may investigate the b-representation $\mathrm{Re}\mathscr{R}(s, b)$ and see whether or not it is peripheral.

In the case of class II models the answer is obviously positive. Since Im R(s, t) is assumed to be peripheral and since the phase (Eq. (41), (42)) is independent of t, Re R(s, t) is necessarily peripheral. But this case is perhaps the least interesting as we shall see in Section V. The real parts for class I and class III models are very similar for sufficiently small values of r_0 (see figure 5). By numerically performing the relevant Bessel transforms we have found that the b-representations of these real parts are almost never dominated by the $b \sim r$ impact parameters and that even the qualitative shape of $\mathrm{Re}\mathscr{R}(s, b)$ depends in a fairly sensitive way on the parameters used as well as on the energy. As an example, we show in figure 6 the b-representations of the real parts of $\Delta\lambda = 0$ and $\Delta\lambda = 1$ negative signature amplitudes corresponding to a class III model. The

parameters chosen are the same as in figure 5. It is evident that the $b \sim r \sim 5$ BeV^{-1} region is not dominant. In fact, in this particular example there seems to be a minimum at $b \sim r$, but this is presumably an accident since it does not occur for other values of the parameters. The b-representations of Re R for class I models are qualitatively similar to those of class III.

We therefore conclude that if R(s, t) possesses its asymptotic phase at finite energies, Re R (s, t) is usually not dominated by the peripheral impact parameters (except in class II models).

V. The Real Part of R(s, t): Applications

In order to test the various possible schemes outlined in the previous section we have to isolate the real parts of specific helicity amplitudes. In a few cases this can be done with some confidence but, in most cases, it is very difficult to determine the real part of a given amplitude.

The one case in which we, more or less, know[3,18] Re R(s, t) is the $\Delta\lambda = 1$ R-amplitude in processes such as $\pi N \to \pi N$, $\pi N \to \eta N$ and $KN \to KN$ at energies of several BeV's. The elastic polarizations, as well as the inelastic differential cross sections indicate that, for $C = -1$, t-channel exchanges (ρ, ω and their associated cuts) —

$$\text{Re } R_1^-(s, t) \sim \text{Im } R_1^-(s, t) \tan \frac{\pi\alpha(t)}{2} \tag{51}$$

while for $C = +1$ exchanges (f^o, A_2 and their associated cuts) —

$$\text{Re } R_1^+(s, t) \sim -\text{Im } R_1^+(s, t) \cot \frac{\pi\alpha(t)}{2} \tag{52}$$

where $\alpha(t) \sim 0.5 + t$. In both cases $\mathrm{Im}\, R_1(s,t)$ includes the $J_1(r\sqrt{-t})$ factor which vanishes around $t \sim -0.5$ BeV^2. Consequently[3], $\mathrm{Re}\, R_1^-(s,t)$ has a double zero and $\mathrm{Re}\, R_1^+(s,t)$ has no zero[19] at $t \sim -0.5$.

This behavior may correspond to class I models (Eqs. (37) and (38)) or to class III models, provided that the parameter r_0 is sufficiently small and the influence of the extra terms in Eq. (50) is numerically unimportant. At present, we cannot distinguist between these two possibilities.

In contrast with the $\Delta\lambda = 1$ amplitudes, we know very little about the real part of the $\Delta\lambda = 0$ amplitudes in the same processes. Assuming that $\mathrm{Im}\, R_0^-$ and $\mathrm{Im}\, R_1^-$ are given, at present energies, by Eq. (4) and that $\mathrm{Re}\, R_1^-$ is given by Eq. (51) one can try to use polarization measurements for $\pi^- p \to \pi^0 n$ in order to isolate[20] $\mathrm{Re}\, R_0^-(s,t)$ in this process. Alternatively, we may take $\mathrm{Re}\, R_0^-$ and $\mathrm{Re}\, R_1^-$, as given by our various classes of models, predict the $\pi^- p \to \pi^0 n$ polarization and compare it with the data. Among our different models, class II models are already ruled out by the observed behavior of $\mathrm{Re}\, R_1^-$ and class I models cannot make definite predictions for $\mathrm{Re}\, R_0(s,t)$ since we do not know which mechanism eliminate the poles in $\tan \frac{\pi\alpha(t)}{2}$ or $\cot \frac{\pi\alpha(t)}{2}$. The type (a) mechanism of Section IV is unacceptable here (since the zeroes of $J_0(r\sqrt{-t})$ do not coincide with these poles). The other possibility, namely — the type (b) mechanism of Section IV is very reasonable but it leaves us with an unpredictable real part.[21] The only exercise left for us is therefore to assume the class III model and see whether it reproduces the $\pi^- p \to \pi^0 n$ polarization.

Using the same approximate integration[17] of Eq. (49) that we have used in Section IV we now assume:

$$\mathrm{Im}\, R_0^-(s,t) = C_0 s^{\alpha(t)} J_0(r_0 \log s \sqrt{-t}) \tag{53}$$

$$\text{Im } R_1^-(s,t) = C_1 s^{\alpha(t)} J_1(r_0 \log s\sqrt{-t}) \tag{54}$$

$$\text{Re } R_0^-(s,t) = C_0 s^{\alpha(t)}\left[\text{Re tan}\frac{\pi\alpha_+(t)}{2} J_0(r_0\log s\sqrt{-t}) - \text{Im tan}\frac{\pi\alpha_+(t)}{2} J_1(r_0\log s\sqrt{-t})\right] \tag{55}$$

$$\text{Re } R_1^-(s,t) = C_1 s^{\alpha(t)}\left[\text{Re tan}\frac{\pi\alpha_+(t)}{2} J_1(r_0\log s\sqrt{-t}) + \text{Im tan}\frac{\pi\alpha_+(t)}{2} J_0(r_0\log s\sqrt{-t})\right] \tag{56}$$

where:

$$\alpha_+(t) = \alpha(t) + i r_0\sqrt{-t} = \alpha_0 + A_0 t + i r_0\sqrt{-t} \quad . \tag{57}$$

We know that:

$$\left(P\frac{d\sigma}{dt}\right)_{\pi^- p \to \pi^o n} = 2\,\text{Im } R_0^* R_1 \quad . \tag{58}$$

Hence

$$\left(P\frac{d\sigma}{dt}\right)_{\pi^- p \to \pi^o n} \sim -2C_0C_1 s^{2\alpha(t)}\,\text{Im tan}\frac{\pi\alpha_+(t)}{2}\left[J_0^2 + J_1^2\right] \tag{59}$$

Equation (59) indicates that the predicted polarization for $\pi^- p \to \pi^o n$ is <u>negative</u>. An explicit calculation using the full expression (Eq. (49)) for the real part confirms this and yields a large negative polarization ($\mathscr{P} \sim -0.7$ at $t \sim -0.5$ for the parameters of figure 5). This contradicts the recent data[22] at 5 and 8 BeV/c which actually showed a large <u>positive</u> polarization for $\pi^- p \to \pi^o n$.

We may therefore conclude that regardless of whether the imaginary part obeys the requirements of class I, II or III, the real part of $R_0^-(s,t)$ does not achieve its asymptotic phase at energies of several BeV's. This conclusion is

consistent with previous analysis of the real part[20] and it confirms the suspicion the $\mathrm{Re}\, R_0(s,t)$ and $\mathrm{Re}\, R_1(s,t)$ have different relations to their respective asymptotic phases. The only way to obtain a positive polarization for $\pi^- p \to \pi^o n$ from Eq. (59) is to assume that the parameter r_0 is negative[23], i.e. that the radius decreases when the energy increases. Such an energy dependence seems to us totally unreasonable. We suspect that Eq. (59) is simply wrong at present energies and we trace its failure to the failure of Eq. (55), i.e. to the failure of $R_0^-(s,t)$ to reach its asymptotic phase.

The polarization in $\pi^- p \to \pi^o n$ is a sensitive test of the various models, since it vanishes at the limit of $r_0 \to 0$ in our class III model, corresponding to a class I model with an exact $\tan \frac{\pi\alpha(t)}{2}$ phase in both helicity amplitudes. Another quantity which vanishes in similar circumstances and which might serve as a guide to the details of the correct model is the observed deviation from various exchange degeneracy predictions. A class I model with no log s terms in C(s) would predict:

$$\frac{d\sigma}{dt}(K^- p \to \bar{K}^o n) = \frac{d\sigma}{dt}(K^+ n \to K^o p) \tag{61}$$

and many similar equalities between other pairs of reactions related to each other by "line-reversal". In many cases, one reaction of the pair is exotic and has a purely real amplitude while the other is nonexotic and has a real as well as an imaginary contribution. The detailed behavior of the real parts of the amplitudes for these processes may produce deviations from the exchange degeneracy equalities. These deviations might, in principle, help us to select the correct class of models. In practice, however, it turns out that the sensitivity of the deviations to the details of the real part is so great that a long time will pass before we can really make

use of them in any reasonable way. The following observation is a good example of this sensitivity.

A class III model, as defined by Eqs. (43), (48) and (49) will usually predict:

$$\frac{d\sigma}{dt}(K^- p \to \bar{K}^o n) \geq \frac{d\sigma}{dt}(K^+ n \to K^o p) \tag{62}$$

or, in general[25]:

$$\left(\frac{d\sigma}{dt}\right)_{\text{nonexotic}} \geq \left(\frac{d\sigma}{dt}\right)_{\text{exotic}} \tag{63}$$

It turns out, however, that this relation may be reversed if we consider a slightly different version of our class III models in which the radius r(s) and the width $\Delta \sim 2\sqrt{A(s)}$ both increase[26] like log s. In that case, the complex J plane structure is even more complicated than that of figure 4 and we may find[27,28]:

$$\left(\frac{d\sigma}{dt}\right)_{\text{exotic}} \geq \left(\frac{d\sigma}{dt}\right)_{\text{nonexotic}} \tag{64}$$

Experimentally, Eq. (64) is more attractive than (63). However, the observed differences between pairs of line reversed reactions may have other contributions[29], and it is very difficult to draw any conclusion from the type of analysis outlined here (except for the fact that the results depend sensitively on the details).

The overall conclusion of our discussion of Re R(s, t) is therefore a statement of theoretical ignorance, with the only exception of the case of $\Delta\lambda = 1$ amplitudes for vector and tensor exchange.

VI. Discussion of Previous Models

The starting point of our analysis in the preceding sections was the assumption that the peripheral impact parameters dominate the imaginary part of R(s, t). Within the framework of this hypothesis we defined our three classes of models. In this section we shall briefly discuss several earlier models for hadronic collisions, and consider their consistency with our basic peripherality assumption as well as their classification into the three classes of models.

(i) The ordinary Regge pole model is, in general, inconsistent with our basic assumption. Although the t-dependence of a typical Regge residue is not fully specified by the model, it must obey several constraints which, in most cases, are inconsistent with the assumption of dominant peripheral impact parameters. A typical example is the tensor-exchange amplitude (such as A_2 or f^o). This amplitude must include a ghost killing α-factor for all values of the helicity change. Its imaginary part must therefore vanish around $t \sim -0.5$ BeV^2. This vanishing usually imposes strong constraints on the impact parameter representation of the same amplitude, and in most cases we find that the peripheral impact parameters are not dominant. An exception to this particular example is the $\Delta\lambda = 1$ amplitude which may turn out to be peripheral (because of the peculiar coincidence between the zeroes of $J_1(r\sqrt{-t})$ and $\alpha(t)$). Our general conclusion is, therefore, that the Regge pole model is inconsistent with our basic assumption, with a few exceptional cases. In those cases this model is obviously a class I model, since the zeroes of the amplitude are fixed while shrinking continues at all energies (see Table I and Section II).

(ii) Regge pole models with "weak cuts"[6] take absorption into account. However, in several cases, the absorption correction is not sufficiently large and,

as a result, the amplitude is not sufficiently peripheral. This is the case for the $\Delta\lambda = 0$ amplitude in elastic πp and Kp scattering, where the "weak cut" model is inconsistent with our basic assumption (and with experiment). In the case of the $\Delta\lambda = 1$ amplitudes the "weak cut" models are certainly adequate. Within our classification, such models belong to class III.

(iii) Regge pole models with "strong cuts"[7] can be consistent with our basic assumption and are usually designed to enhance the relative importance of the peripheral partial waves. In such models the radius increases logarithmically (essentially because of the slope of the input trajectory). The width of the peripheral distribution also increases with energy. At sufficiently high energy (far above our present energies) the "absorbed" region in the b-representation becomes small relative to the radius (in other words, while $(r-\Delta)$ is bounded below, $\Delta/r \to 1$ as $s \to \infty$). This type of model is basically a class III model in our terminology, except that it has an "internal radius" r_1 and an "external radius" r_2 (see figure 7). The first grows with energy like log log s while the second increases logarithmically. The C(s) term in such models involves significant log s factors and the real part approaches its predicted asymptotic phase very slowly. At energies of a few BeV the phase of the "strong cut" model is totally different from its asymptotic value (and for $\Delta\lambda = 1$ vector and tensor exchanges this contradicts the data[3,18]). The impact parameter representation of the real part is peripheral in this model, contrary to our conclusions in Section IV.

(iv) The Dar-Weisskopf absorption model[8] is perfectly consistent with our basic assumption. It is basically a class III model since it has a logarithmically increasing radius. However, this model does not possess the correct asymptotic real part. Its real part is also peripheral.

(v) Complex pole models[12] may be consistent with our basic assumption. This is especially true in those models where the complex poles are viewed merely as a convenient mathematical description of absorptive cuts. Such models belong to our class III and the real parts of their amplitudes are similar to the ones derived in our discussion in Sections IV and V.

VII. The Diffractive Component — P(s, t)

Our entire discussion, so far, was devoted to the properties of the non-diffractive component R(s, t). We now turn to a brief discussion of the P-component. The Pomeron exchange amplitude is qualitatively given in figure 1b by a non-peripheral b-representation. The Pomeron exchange term seems to be structureless[3] for $t < 1$ BeV^2. We therefore assume, for simplicity[30]:

$$\text{Im}\, P(t) = C_P e^{A_P t} \tag{65}$$

This corresponds to a Gaussian distribution in impact parameter:

$$\text{Im}\, \mathscr{P}(b) = \frac{C_P}{2A_P} e^{-b^2/4A_P} \tag{66}$$

A natural way to define the effective radius of the Pomeron exchange term is therefore:

$$r_P = 2\sqrt{A_P} \tag{67}$$

This radius has no simple relation to the radius r which characterizes the R-component of the amplitude. The energy dependence of the functions $C_P(s)$ and $r_P(s)$ (or $A_P(s)$) determines the behavior of Im P(s, t) at high energies, and through it — the behavior of Re P(s, t). Another interesting parameter is the degree of absorption or the "opacity" which is proportional to C_P/A_P. The total cross

section is proportional to $\frac{1}{s}$ Im P(t=0) as $s \to \infty$.

The conventional models for the P-component fall into three categories, when classified in terms of the asymptotic energy dependence of their C_P and r_P parameters.

First category:

$$r_P(s) \xrightarrow[s\to\infty]{} r_{P\infty} \; ; \quad C_P(s) \xrightarrow[s\to\infty]{} C_{P\infty} s \tag{68}$$

$$\text{Im } P(s,t) \xrightarrow[s\to\infty]{} C_{P\infty} e^{r_{P\infty}^2 t/4} \; . \tag{69}$$

In this case the radius approaches a constant at high energies; the total cross section approaches a constant; no shrinking should be observed at high energies; the opacity approaches a constant. In such models the Pomeron term is given by a fixed J-plane singularity. The corresponding real part obeys:

$$\frac{\text{Re } P(s,t)}{\text{Im } P(s,t)} \xrightarrow[s\to\infty]{} 0 \tag{70}$$

This possibility is consistent with the most naive geometrical-optical approach.

Second category:

$$r_P^2(s) \xrightarrow[s\to\infty]{} r_{P0}^2 \log s \; ; \quad C_P(s) \xrightarrow[s\to\infty]{} C_{P\infty} s \tag{71}$$

$$\text{Im } P(s,t) \xrightarrow[s\to\infty]{} C_{P\infty} s^{(1+\frac{1}{4} r_{P0}^2 t)} \tag{72}$$

In this case $A_P(s)$ increases like log s; the total cross section is constant; the diffraction peak shrinks logarithmically; the opacity decrease logarithmically. The Pomeron term represents a moving J-plane singularity. The real part obeys:

$$\frac{\mathrm{Re}\,P(s,t)}{\mathrm{Im}\,P(s,t)} \xrightarrow[s\to\infty]{} -\cot\left[\frac{\pi}{2}\left(1+\tfrac{1}{2}\,r_{P0}^{2}t\right)\right] \tag{73}$$

Third category:

$$r_P(s) \xrightarrow[s\to\infty]{} r_{P0}\log s\,;\quad C_P(s) \xrightarrow[s\to\infty]{} C_{P0}\,s\log^2 s \tag{74}$$

This is the "maximal" case saturating the Froissart bound. If we insert the asymptotic behavior of Eq. (74) into our canonical diffractive form (Eq. (65)) we find that, for $t < 0$, the amplitude decreases with energy faster than any power of s. Such a possibility is unacceptable[31] and we have to assume that the impact parameter representation $\mathrm{Im}\mathscr{P}(b)$ is different than the Gaussian of Eq. (66). The simplest alternative which is consistent with Eq. (74) is the model of a completely absorbing disk with a logarithmically increasing radius[32]. In this case the total cross section grows like $\log^2 s$, the slope of the diffraction peak increases like $\log^2 s$ and the opacity is constant. The corresponding J-plane structure involves complex singularities[32].

Other possibilities exist, of course, but they are theoretically less appealing and we shall not study them here.

It is clear that the two crucial experimental quantities that are needed for determining $C_P(s)$ and $r_P(s)$ are, respectively, the total cross section and the slope of the diffraction peak at high energies. The present data from Serpukhov[33] and from the CERN Intersecting Storage Rings[34] are confusing in this respect since they seem to indicate that $C_P(s)$ increases while $r_P(s)$ does not. That would mean that the opacity increases, a process which cannot continue indefinitely since the

opacity has a fixed upper limit corresponding to full absorption. We hope that the next few months will settle this issue and will help us select the correct category of models.

VIII. Summary, Conclusions and Several Open Problems

We have presented here a discussion of a number of rather technical points related to the behavior of hadronic two-body scattering amplitudes at high energies. We did not try to reach decisive conclusions on most issues. Rather, we have tried to outline the different possibilities in every case, and to suggest experimental tests which will help us select the right solutions. A few general concluding remarks should help us to separate the technical details to which much of our previous discussion has been devoted from the important qualitative problems.

Our first observation is that all evidence[3] points in the direction of a non-Pomeron component R(s, t) whose imaginary part is dominated by the peripheral impact parameters. This was our starting point in the present paper.

Our next remark was that a peripheral imaginary part is inconsistent with indefinite shrinking of inelastic amplitudes and with an asymptotically constant effective radius. We have to abandon at least one of the three assumptions as $s \to \infty$, i.e. either the peripheral impact parameters cease to dominate or the shrinking of inelastic differential cross sections stops or the radius increases indefinitely. These three options lead to three families of models (described in Section II) which in one way or the other incorporate the many earlier versions of the absorption model. Simple feasible experiments (mentioned in Section III) should help us decide in the near future between these three possibilities.

Our third observation is that, regardless of which of the many possibilities of Section IV becomes true, the real part of R(s, t) has no reason to be dominated by the peripheral impact parameters and, in general, it is not dominated by them. This is certainly true when the real part approaches its asymptotic phase at an early energy.

Concerning the details of the real part — we basically have two possibilities. It may reach its asymptotic behavior very rapidly at relatively low energies or it may reach it very slowly (with nonleading terms which are smaller than the leading term only by factors of log s). If the asymptotic phase is reached at an early stage, the general features of the real part are insensitive to the detailed energy dependence of the radius, as long as the latter does not increase too fast. The example shown in figure 5 demonstrates this point. If, however, the approach to the asymptotic phase is slow and the present energy domains are below the asymptotic region we remain completely ignorant with respect to the real part. We have remarked that for vector and tensor exchanges, $\Delta\lambda = 1$ amplitudes reach their asymptotic phase very early while $\Delta\lambda = 0$ amplitudes do not seem to do so. It has been spectulated[3] that this follows from the fact that the Regge pole term in $\mathrm{Im}\, R_{\Delta\lambda = 0}$ cannot be peripheral and require a large cut contribution which induces log s factors in the energy dependence C(s). Even if this is true, it sounds like an accident which requires explanation.

The energy dependence of the two radii — r(s) and $r_P(s)$ — is extremely important. The first of these radii controls most of the striking features of inelastic differential cross-sections. The second is relevant both to our understanding of diffraction scattering and, through unitarity, to our understanding of the multihadronic final states which dominate the total cross section at high energies.

Notice that the correlation between these radii is far from clear. Intuitively, we might suspect that if one of them grows with energy, so does the other. However, one can think of models in which, for instance, the diffractive radius r_P stays constant while the nondiffractive radius r increases. In such a case, as the energy increases, the decreasing contributions of inelastic two-body final states may come from larger and larger impact parameters within the "grey fringe" of the hadron. In any event, the high energy behavior of the radii should be found soon from accurate measurements of elastic differential cross sections (where the slope determines r_P and the crossover point determines r).

We have often referred to the $s \to \infty$ behavior of various quantities. It is conceivable that some of these quantities (such as one of the radii) grow steadily until a certain energy and only then begin to approach a constant. Such a behavior might affect our conclusions, especially those related to the real part. The real part of R(s, t) was analysed in Section IV by using asymptotic forms for Im R(s, t) and essentially substituting them in fixed-t dispersion relations. In this case the main influence on the real part at a given energy comes from the imaginary part in a region centered around the same energy. Consequently, if r(s) grows logarithmically until, say, $s = 1000$ BeV^2 and then slowly becomes constant, we may safely ignore its $s > 1000$ behavior when discussing the real part at, say, $s = 200$ BeV^2. In that sense, when we talk about the $s \to \infty$ behavior we really refer to some finite energy domain. We should then believe the conclusions for energies which are not too close to the higher energy end of this domain. We have performed several numerical calculations checking the sensitivity of the real part to such a possibility and found that when "$s \to \infty$" for Im R(s, t) is defined as some energy s_{max} the conclusions regarding the real part are certainly safe for $s \lesssim \frac{1}{2} s_{max}$ assuming that no violent changes occur anywhere.

We have noticed two specific examples of quantities which are extremely sensitive to otherwise minor details. These are the polarization in $\pi^- p \to \pi^o n$ and the deviations from the exchange degeneracy predictions for line reversed reactions. We feel that, at present, we are far from reaching the stage in which we would like to use such sensitive probes in order to settle fine details. However, when all the relevant parameters and energy dependences are experimentally decided, we may return to these quantities as a tool for pinpointing such details.

Meanwhile, we should continue to analyze existing data, testing our various classes of models as well as our basic peripherality assumption, hoping to get some better understanding of the nature of hadronic collisions.

We thank many colleagues, particularly G. Ringland and R. Roskies, for helpful comments.

Footnotes and References

1. H. Harari, Phys. Rev. Letters 20, 1395 (1968); P. G. O. Freund, Phys. Rev. Letters 20, 235 (1968).

2. R. Dolen, D. Horn and C. Schmid, Phys. Rev. 166, 1768 (1968).

3. H. Harari, Ann. of Phys. (N.Y.) 63, 432 (1971); H. Harari and M. Davier, Phys. Letters 35B, 239 (1971); H. Harari, Phys. Rev. Letters 26, 1400 (1971); H. Harari, SLAC-PUB-914, to be published in the Proceedings of the Tel-Aviv Conference on Duality and Symmetry in Hadron Physics, 1971.

4. The idea of dominant peripheral partial waves is an old one in particle physics. It is even older in other fields such as nuclear physics. Many versions of absorption models for hadronic processes have been proposed in the last ten years. Some representative references are listed below.

5. M. J. Sopkovich, Nuovo Cimento 26, 186 (1962); A. Dar, M. Kugler, Y. Dothan and S. Nussinov, Phys. Rev. Letters 12, 83 (1964); A. Dar and W. Tobocman, Phys. Rev. Letters 12, 511 (1964); K. Gottfried and J. D. Jackson, Nuovo Cimento 34, 735 (1964); L. Durand and Y. T. Chiu, Phys. Rev. Letters 12, 399 (1964).

6. R. C. Arnold, Phys. Rev. 153, 1523 (1967); R. C. Arnold and M. L. Blackmon, Phys. Rev. 176, 2082 (1968); M. Blackmon, Proceedings of the Argonne Symposium on Polarization, 1970; A. Capella and J. Tranh Than Van, Nuovo Cimento Letters 1, 321 (1969).

7. F. S. Henyey, G. L. Kane, J. Pumplin and M. Ross, Phys. Rev. 182, 1579 (1969); M. Ross, Proceedings of the Regge Pole Conference, Irvine, 1969; M. Ross, F. S. Henyey and G. L. Kane, Nuclear Phys. B23, 269 (1970).

8. A. Dar, T. L. Watts and V. F. Weisskopf, Nuclear Phys. B13, 477 (1969); A. Dar, Proceedings of the Columbia Conference, 1969.

9. See, e.g. I. S. Gradshteyn and I. M. Ryzhik, Table of Integrals, Series and Products, Academic Press, 1965.

10. Throughout the paper we measure s in units of s_0, namely — all log s or s^α terms stand for $\log(s/s_0)$ or $(s/s_0)^\alpha$, respectively.

11. Whenever we assume an energy dependence of the form s^α we allow, without writing so explicitly, multiplicative powers of log s. All our statements on power behavior in s should be considered modulu such log s terms.

12. For a review of the connection between Regge cut models and models involving complex poles see e.g. F. Zachariasen, CERN preprint, 1971, and references therein.

13. This crude estimate is based on the variation of the slope of the pp diffraction peak between 5 and 70 BeV. This slope represents a different radius than the one discussed here, but it is reasonable to assume, as a first approximation, that the radius of the P-amplitude and radius of the R-amplitude have a similar growth rate (if they both grow). This gives $r_0 \sim 0.2$ GeV^{-1}. See, however, our discussion in Section VIII on the relation between the two radii.

14. N. N. Khuri and T. Kinoshita, Phys. Rev. 137B, 720 (1965).

15. In spite of the obvious necessity of introducing contributions of cuts in the complex J-plane, we believe that the t-channel quantum numbers of the exchanged objects are simple, in most cases, and that to a good approximation the combined pole-cut contribution has simple crossing properties. (For instance, the ρ - Pomeron cut is presumably odd under s $\longrightarrow$ u crossing, etc.) Another complication arises in high spin cases where the s-channel helicity flip and

the u-channel helicity flip are not simply related at high energy. (See the discussion of G. Berlad, G. Eilam and R. Stokhamer, Technion preprint, 1971.) In such cases we presumably have to consider separately the $s \to \infty$ and the $s \to -\infty$ limits. A third problem, which is much simpler to handle, is the case where both even and odd signatured exchanges are present (as in $K^- p \to \bar{K}^0 n$). In this case we should consider separately the real parts of the two different signatures, and add them at the end of the analysis.

16. For a given value of r_∞, $J_{\Delta\lambda}(r_\infty \sqrt{-t})$ vanishes at different t-values for different values of $\Delta\lambda$. Since $\alpha(t)$ is presumably independent of $\Delta\lambda$, this subtle calcellation mechanism can, at best, occur for one specific value of $\Delta\lambda$.

17. Using the symmetry properties of the integral under $\phi \leftrightarrow -\phi$, Eq. (49) can be written as

$$\mathrm{Re}\, R_0^-(s,t) = \frac{C_0}{\pi} s^{\alpha_0 + A_0 t} \int_0^\pi \left\{ \mathrm{Re}\tan\left[\frac{\pi}{2}(\alpha_0 + A_0 t + i r_0 \sqrt{-t}\sin\phi)\right] \mathrm{Re}\, s^{i r_0 \sqrt{-t}\sin\phi} \right.$$

$$\left. - \mathrm{Im}\tan\left[\frac{\pi}{2}(\alpha_0 + A_0 t + i r_0 \sqrt{-t}\sin\phi)\right] \mathrm{Im}\, s^{i r_0 \sqrt{-t}\sin\phi} \right\} d\phi$$

for $s \to \infty$ we may use the approximation $\phi \sim \frac{\pi}{2}$ in the argument of the tangents. This leads to a combination of a J_0 Bessel function and an H_0 Struve function (see reference 9). The latter is equivalent to a J_1 Bessel function, within the approximation used here, and Eq. (50) follows.

18. R. J. N. Phillips and G. A. Ringland, Nuclear Phys. B, to be published.

19. Needless to say, we cannot guarantee that $\alpha(t)$ and $J_1(r\sqrt{-t})$ vanish exactly at the same point. We do know, however, that they both vanish around $t \sim -0.5$ and that $\mathrm{Re}\, R_1^+(s,t)$ is fairly smooth in this region, hinting that the pole of $\cot\frac{\pi\alpha(t)}{2}$ is washed away by the zero of $J_1(r\sqrt{-t})$.

20. G. A. Ringland and D. P. Roy, Rutherford Laboratory preprint, 1971.

21. The results of reference 20 seem to correspond to this possibility.

22. O. Guisan et al., to be published.

23. This has been recently recognized by N. Barik et al., UC Riverside preprint, 1971 and by B. R. Desai, Seattle preprint, 1971. These authors discuss complex pole models which resemble our class III models in Section IV. They find a negative value for r_0.

24. P. Sonderegger et al., Physics Letters 20, 75 (1966).

25. In order to see this we may replace the complex cut by a continuous superposition of complex conjugate pairs of poles located at J and J* with effective residues β and β^*, where

$$\beta = \frac{1}{\sqrt{(J-\alpha_+)(J-\alpha_-)}} \frac{1}{\sin \pi J} .$$

Neglecting the interference between different pairs of poles, we find that $(\frac{d\sigma}{dt})_{\text{exotic}} = (\beta + \beta^*)^2$ while $(\frac{d\sigma}{dt})_{\text{nonexotic}} = (\beta \cos \pi J + \beta^* \cos \pi J^*)^2 + (\beta \sin \pi J + \beta^* \sin \pi J^*)^2$. Some simple algebra then leads to the relation (63).

26. So far we have always assumed that for class III models $A(s) \xrightarrow[s \to \infty]{} A_0 \log s$. Needless to say, other powers of log s could be present in A(s) but all our qualitative conclusions until this point were not sensitive to this possibility. Here we find, however, that $A(s) \to A_0 (\log s)^2$ may yield a drastically different result.

27. For each value of t, the cut from α_+ to α_- (figure 4) will now be "smeared" along the real J-axis. Strong interference terms may result between contributions of different values of Re J. A close inspection shows that it is actually

very likely that these terms will reverse the inequality (63) and make the exotic cross section larger than the nonexotic. This is the case in the work of reference 28 where the inequality (64) has been obtained.

28. D. P. Roy et al., Phys. Letters 34B, 512 (1971).

29. Deviations from the predicted equality between exotic and nonexotic line-reversed pairs of reactions, could come from several sources: (i) there may be a small residual imaginary part in the exotic reactions, (ii) the degeneracy between the energy dependence of the even and odd signatured exchanges may be broken; (iii) low lying trajectories or cuts (especially double particle exchange contributions) may produce strong deviations at low energies, (iv) at present energies, the phase of the $\Delta\lambda = 0$ amplitude is completely different from the asymptotic phase.

30. The data actually indicates that an amplitude of the form $C\, e^{At + Bt^2}$ might be more appropriate. However, our qualitative remarks in this section will not be changed by the presence of the extra term and we therefore ignore it at this stage.

31. See e.g. R. J. Eden, High Energy Collisions of Elementary Particles, Cambridge University Press, 1967.

32. H. Cheng and T. T. Wu, Phys. Rev. Letters 24, 1456 (1970); J. Finkelstein and F. Zachariasen, Phys. Letters 34B, 631 (1971); J. R. Fulco and R. L. Sugar, UCSB preprint, 1971.

33. G. G. Benznogikh et al., Phys. Letters 30B, 274 (1969) and reports to the Amsterdam Conference, 1971.

34. M. Holder et al., Phys. Letters 35B, 355 (1971) and reports to the Amsterdam Conference, 1971.

Table I

Summary of Properties of the Three Classes of Models

	$r(s) \xrightarrow[s \to \infty]{}$	$A(s) \xrightarrow[s \to \infty]{}$	Position of Dips	Shrinkage	Dominance of Peripheral Impact Parameter
Class I	r_∞	$A_0 \log s$	fixed	yes	no
Class II	r_∞	A_∞	fixed	no	yes
Class III	$r_0 \log s$	$A_0 \log s$	moving	yes	yes

Figure Captions

Figure 1: (a) Schematic representation of Im $\mathscr{R}(b)$. The dominant impact parameters are centered around $b \sim r$.

(b) Schematic representation of Im $\mathscr{P}(b)$. All impact parameters $b \leq r_P$ contribute significantly.

Figure 2: Impact parameter representation Im $\mathscr{R}(b)$ for $r = 5$ BeV^{-1}, $A = 2$ BeV^{-2}. The two curves show the explicit expression (Eq. (5)) and the approximate expression (Eq. (7)). The approximation is extremely good (although it necessarily breaks at $b = 0$). A realistic value of A at $p_L = 5$ GeV/c is $A = 1.3$ BeV^{-2} (see reference 3), well below the value which we have arbitrarily chosen here. For $A = 1.3$ the approximation of Eq. (7) is even better than the one shown in the figure.

Figure 3: Impact parameter representation Im $\mathscr{R}(b)$ for $r = 5$ BeV^{-1}, $A = 1, 4, 8$ BeV^{-2}, using Eq. (5). For sufficiently large values of A we lose the dominance of the peripheral impact parameters. This is the case at high energies according to class I models.

Figure 4: Class III models can be described by complex conjugate pair of moving branch points $\alpha_\pm = \alpha_0 + A_0 t \pm i r_0 \sqrt{-t}$. The relevant complex cut stretches from α_+ to α_- and it moves as a function of t. Assuming $\alpha_0 = 0.5$, $A_0 = 1$, $r_0 = 0.2$, this complex J-plane structure is shown. All units are in BeV.

Figure 5: A comparison between the real parts obtained in class I and class III models. We assume $\mathrm{Im}\, R^-_{\Delta\lambda}(s,t) = s^{\alpha(t)} e^{ct} J_{\Delta\lambda}\left[(r_1 + r_0 \log s)\sqrt{-t}\right]$ and $s = 8$; $\alpha(t) = 0.5 + t$; $c = -0.3$ (in order to duplicate the t-dependence of Im R in $K^{\pm}p$ scattering; see reference 3); $r_1 = 5\ \mathrm{BeV}^{-1} = 1$ fermi; $r_0 = 0.2$ (see footnote 13). All units are in BeV. We then compute $\mathrm{Re}\, R^-_{\Delta\lambda}(s,t)$ twice. Once by pretending that r(s) is constant, thus multiplying the above expression for Im R by $\tan\frac{\pi\alpha(t)}{2}$. These are the solid curves (for $\Delta\lambda = 0, 1$). We then compute the real part using the full Eq. (49) and its analogous expression for $\Delta\lambda = 1$. The resulting curves are the dashed curves. We see that the differences between the curves are fairly small. A similar exercise for $R^+(s,t)$ reveals larger differences, particularly around $t \sim -0.5$ where $\cot\frac{\pi\alpha(t)}{2}$ has a pole while $\cot\frac{\pi\alpha_+(t)}{2}$ does not. The results for R^+ are extremely sensitive to the chosen value of r_0 and to additional log s terms in the energy dependence.

Figure 6: The b-representation of $\mathrm{Re}\, R^-_0$ and $\mathrm{Re}\, R^-_1$ for a class III model using the parameters described in figure 5 (except that $s = 5$). In both cases Re $\mathscr{R}(b)$ is not dominated by the peripheral impact parameters.

Figure 7: Schematic representation of Im $\mathscr{R}(b)$ in a Regge pole model with "strong cuts". The "external radius" $r_2(s) \xrightarrow[s\to\infty]{} \log s$. The "internal radius" $r_1(s) \xrightarrow[s\to\infty]{} \log\log s$. Hence $r_1/r_2 \to 0$ and the "absorbed region" eventually becomes small relative to the width $(r_2 - r_1)$.

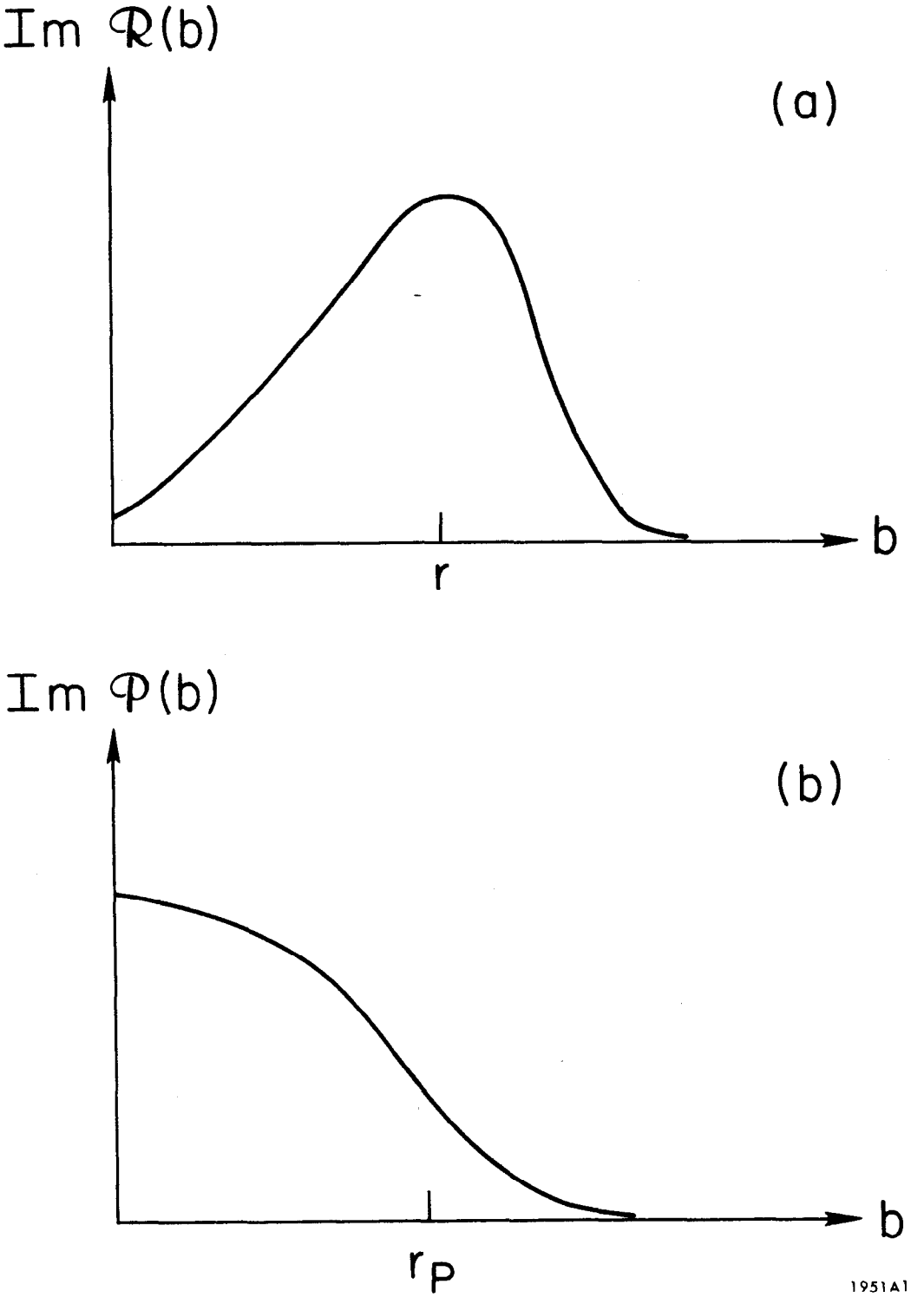

Fig. 1

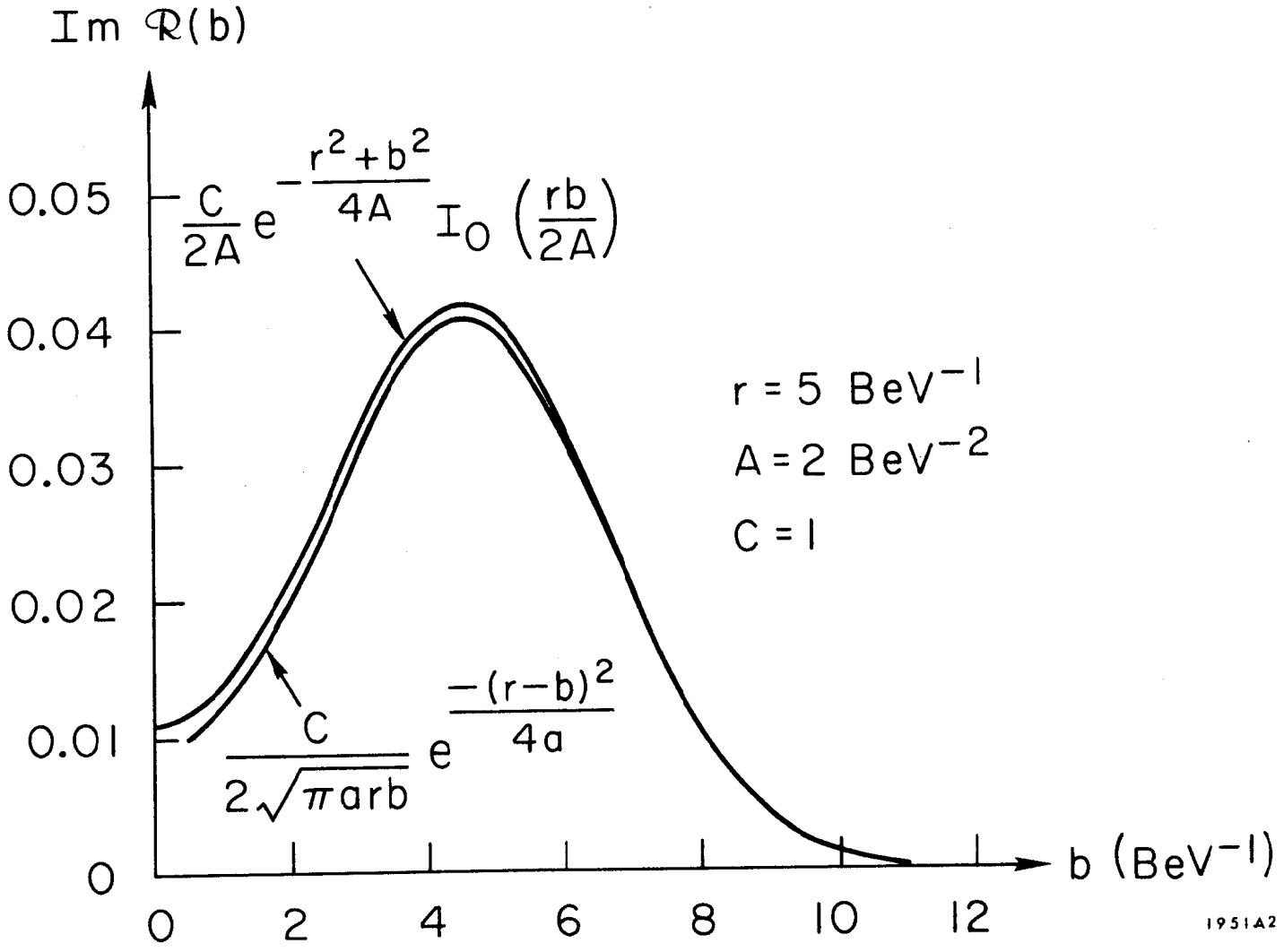
Im ℛ(b)
0.05
0.04
0.03
0.02
0.01
0
$\frac{C}{2A} e^{-\frac{r^2+b^2}{4A}} I_0\left(\frac{rb}{2A}\right)$
$\frac{C}{2\sqrt{\pi arb}} e^{\frac{-(r-b)^2}{4a}}$
r = 5 BeV^{-1}
A = 2 BeV^{-2}
C = 1
0
2
4
6
8
10
12
b (BeV^{-1})
1951A2

Fig. 2

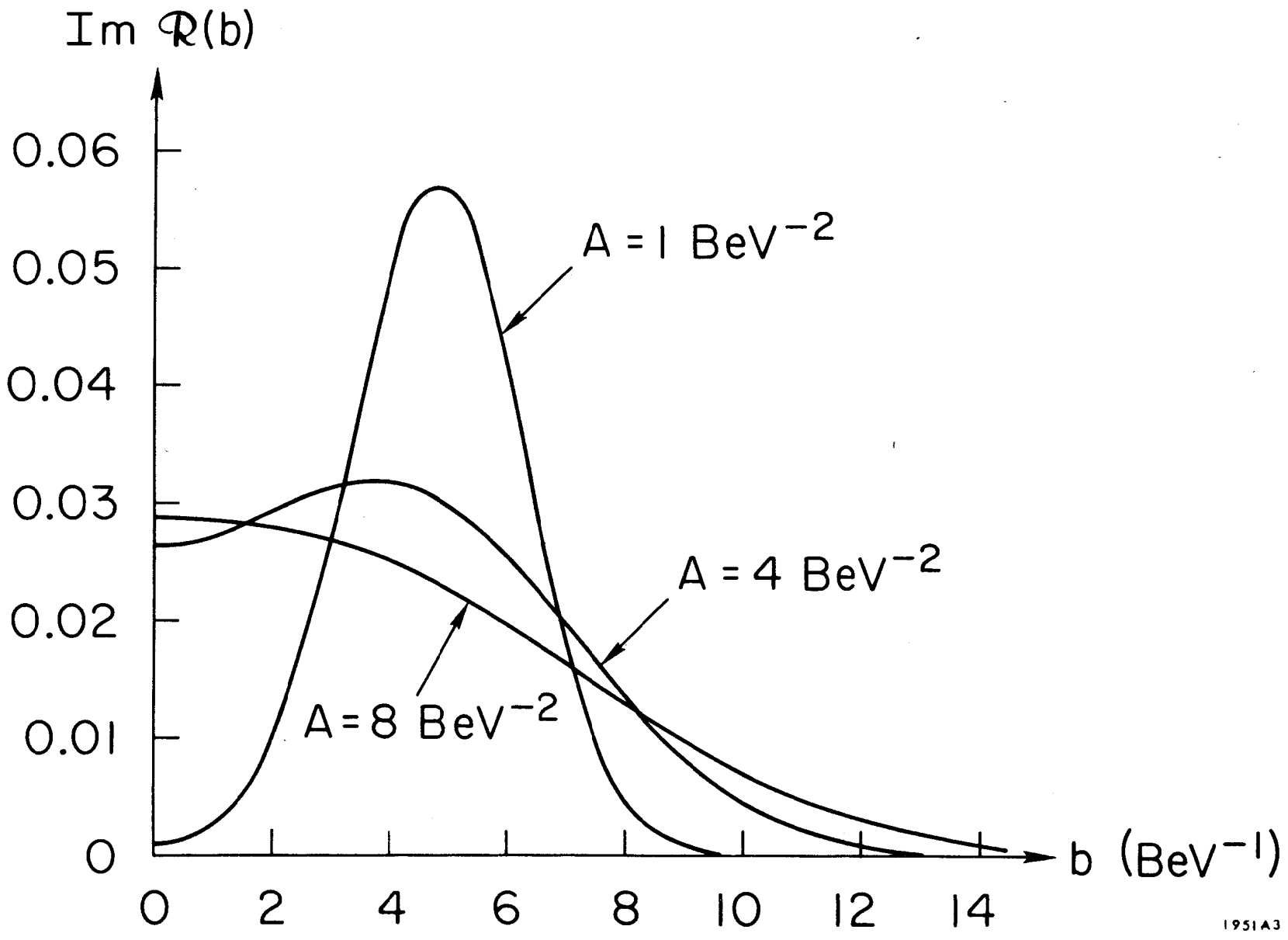
Im $\mathcal{R}(b)$
0.06
0.05
0.04
0.03
0.02
0.01
0
A = 1 BeV^{-2}
A = 4 BeV^{-2}
A = 8 BeV^{-2}
0
2
4
6
8
10
12
14
b (BeV^{-1})
1951A3

Fig. 3

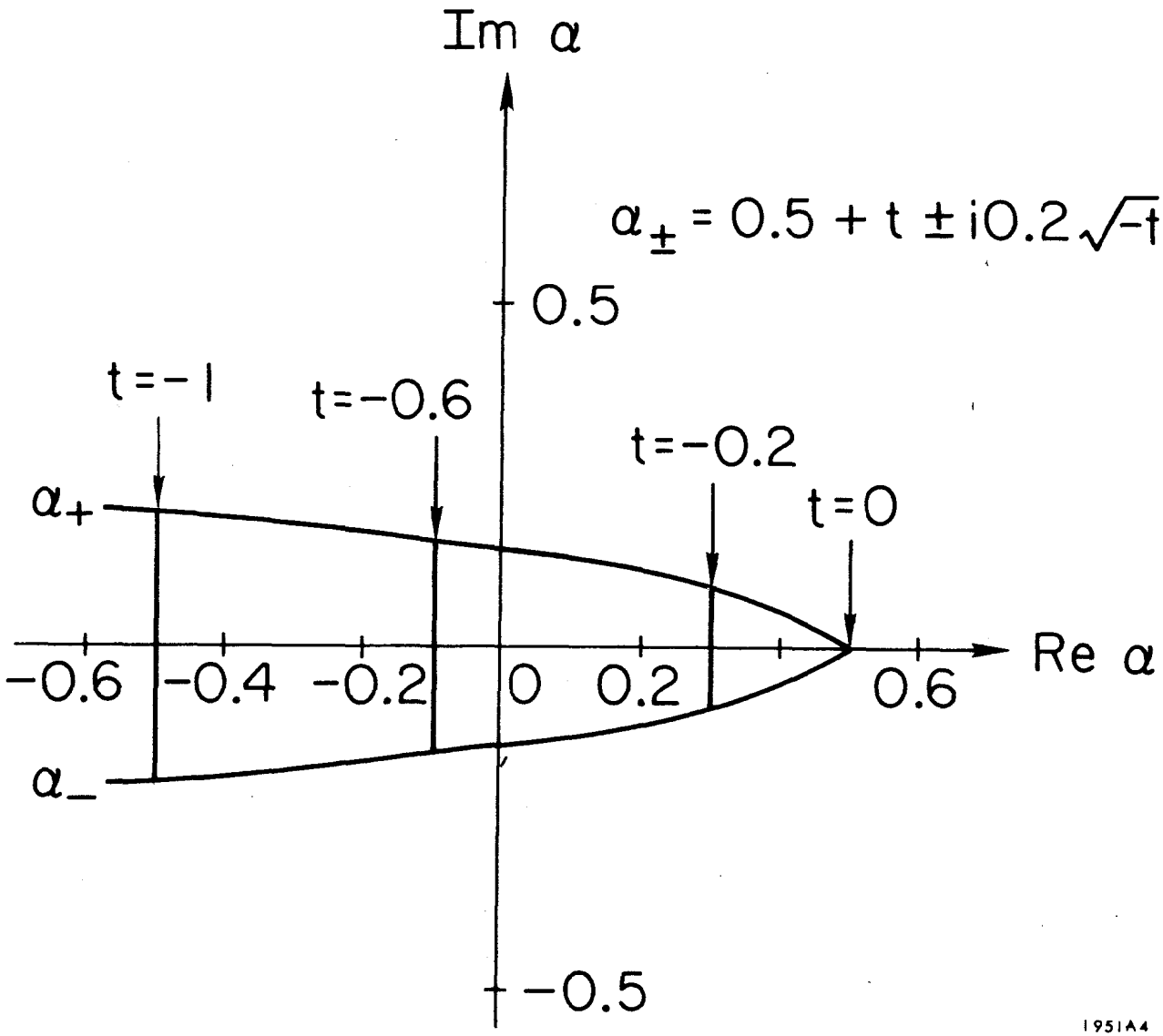
Im α
$\alpha_{\pm} = 0.5 + t \pm i0.2\sqrt{-t}$
0.5
t=-1
t=-0.6
t=-0.2
t=0
α_+
α_-
-0.6
-0.4
-0.2
0
0.2
0.6
Re α
-0.5
1951A4

Fig. 4

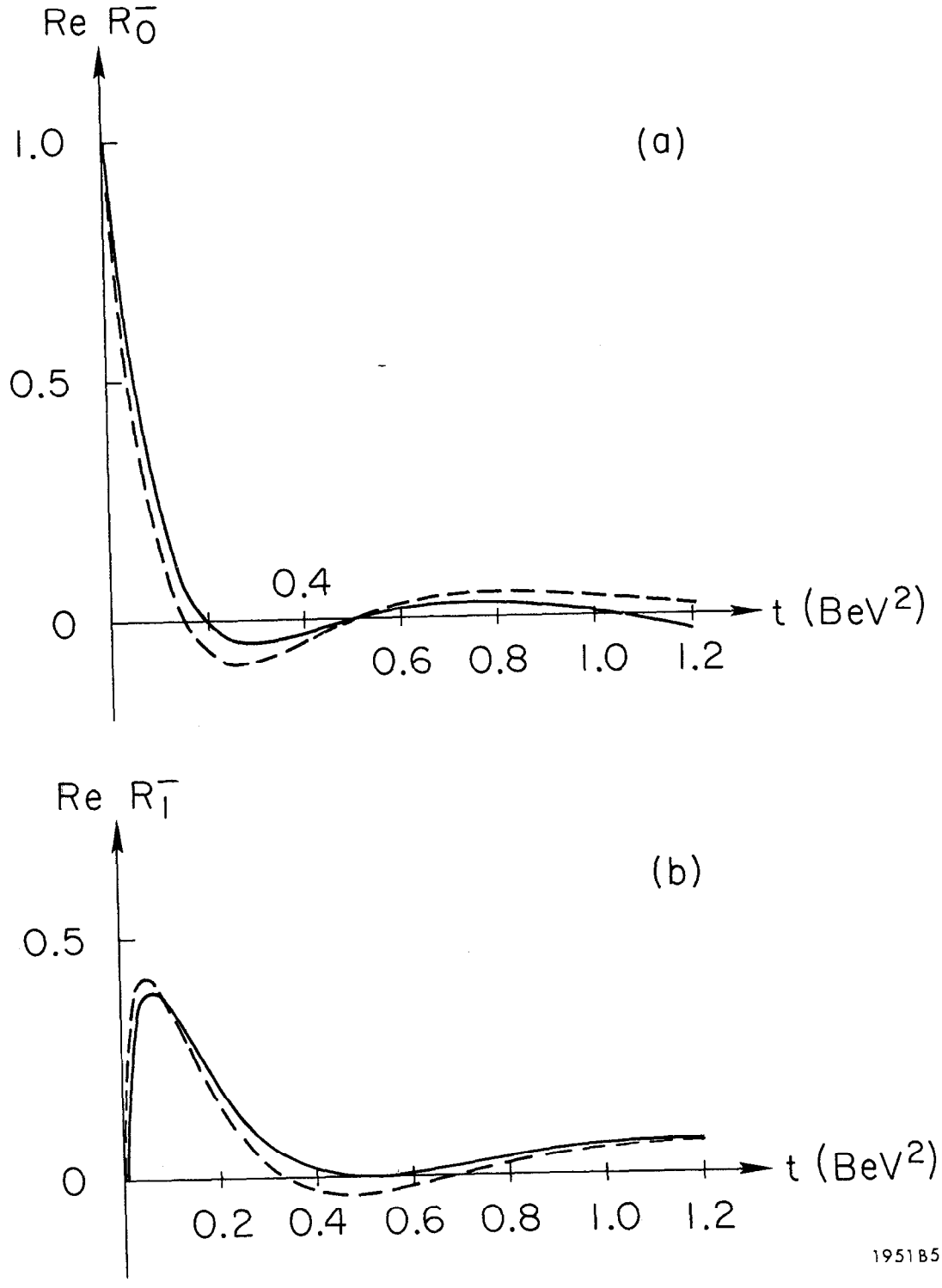
Re R_0^-
1.0
0.5
0
(a)
0.4
0.6
0.8
1.0
1.2
t (BeV^2)
Re R_1^-
(b)
0.5
0
0.2
0.4
0.6
0.8
1.0
1.2
t (BeV^2)
1951B5

Fig. 5

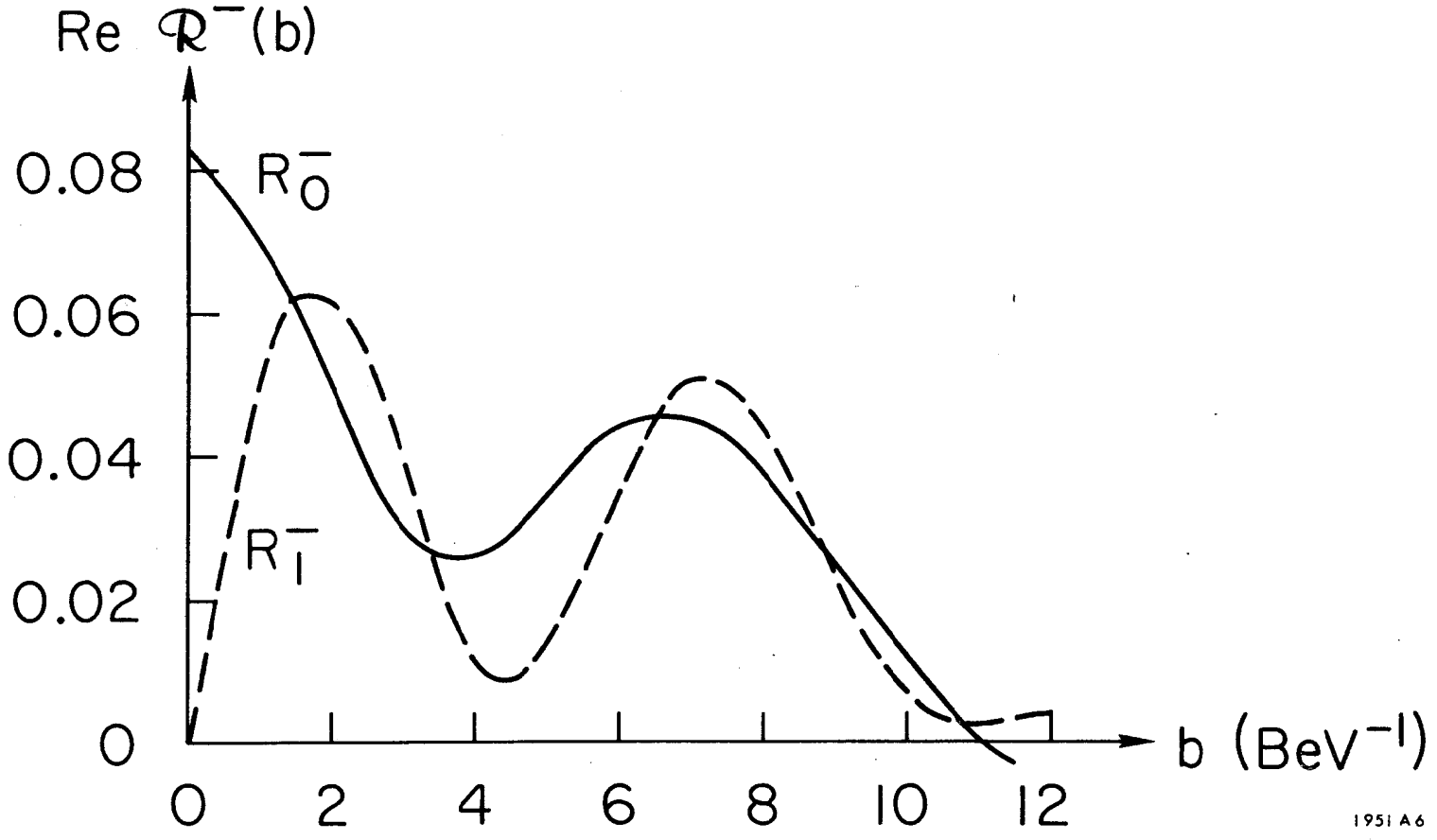

Fig. 6

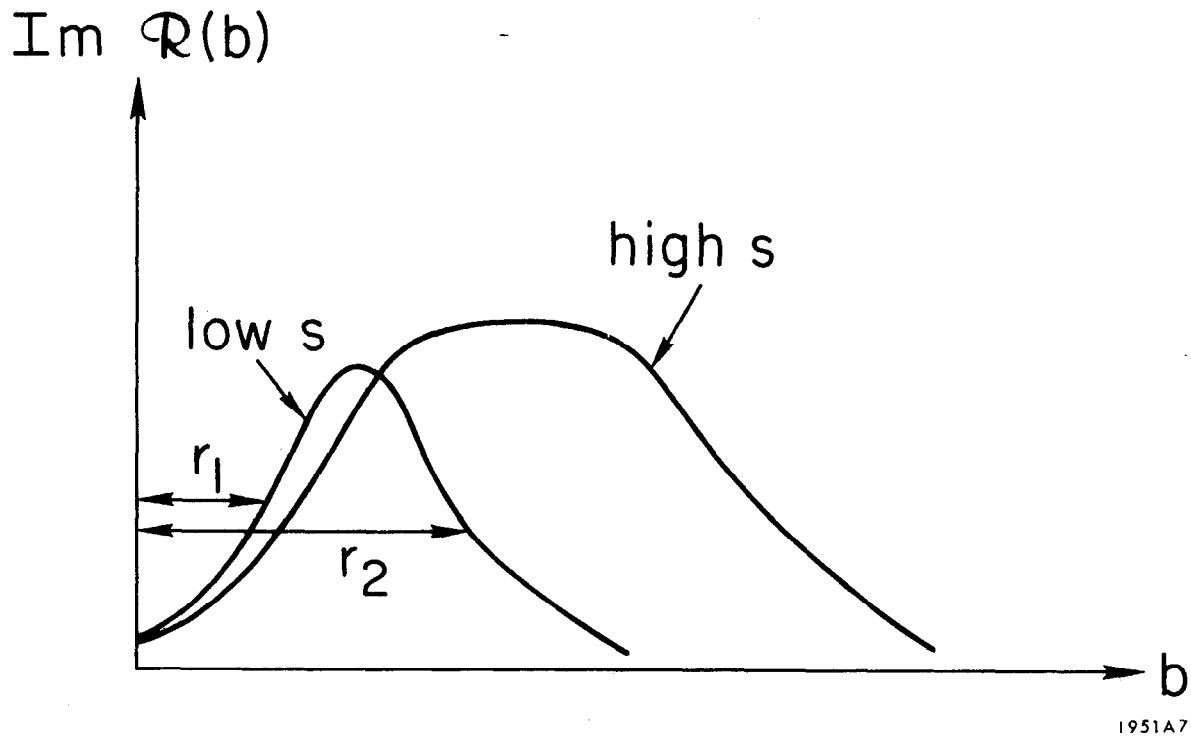

Fig. 7